Free Convection of Al_2O_3 and TiO_2 Nanofluids in Enclosure with Two Models of Thermal Conductivity

Manal AL-Hafidh, Ph.D
Department of Mechanical Engineering
University of Baghdad
College of Engineering

ABSTRACT
This paper presents a numerical study of natural convection of nanofluids contained in horizontal cylindrical annular enclosure filled with porous media and subjected to uniform heat flux along the inner cylinder wall. Governing parameters of the problem under study are the modified Rayleigh number Ra ($10 \leq Ra^* \leq 500$) and the solid volume fraction of nanoparticles ($0 \leq \varphi \leq 0.3$. Two types of nano-particles are taken into consideration Al_2O_3 and TiO_2 with water as the based fluid. Two models are used for calculating the effective viscosity and thermal conductivity of nanofluids. The finite difference approximation and the MATLAB-7 program are used to obtain the results. It is found that Adding 0.5 percent of TiO_2 particles cause to increase the value of the local Nu number to 4.128 for model 1 and to 3.748 for model 2**.** Adding Al_2O_3 particles of 0.5 percent volume fraction cause an increase the local Nu to 4.988 for model 1 and to 4.542 for model2**.** A maximum value of the average Nu of TiO_2 nanofluid is equal 16.446 for model1 with φ=0.5 and Ra^* =500, while Nu equal 4.54 for model 2. A maximum value of the average Nu of 18.0007 for Al_2O_3 nanofluid for model 1 and 5.004 for model 2 is obtained with φ=0.5 and Ra^* =500. A correlation of Nu with Ra^* and φ is obtained for Al_2O_3 nanofluid and TiO_2 nanofluid model 1.

General Terms
Cp: Specific heat at constant pressure (kJ/kg ^{o} C), g: Acceleration due to gravity (m/s^2), kf: Thermal conductivity of the fluid (W/m K), ks: Thermal conductivity of the solid (W/m K), keff.: Effective thermal conductivity of the porous media (W/m K), K: Permeability (m^2), l: Cylinder length (m), L:Dimensionless cylinder length, Nu1: Local Nusselt number on the inner cylinder, Nu2: Local Nusselt number on the outer cylinder, Nu_{in}: Average Nusselt number on the inner cylinder, $Nu_{out:}$ Average Nusselt number on the outer cylinder, p: Pressure (N/m2), q: Local heat flux (m), r: Radial coordinate (m), R: Dimensionless radial coordinate, Ra*: Modified Rayleigh number, Rr: Radius ratio, S: Fin pitch (m), T: Temperature (K), t: time (s), ur,uϕ, uz: velocity component in r,ϕ and z - direction (m/s), Ur, Uϕ, Uz: Dimensionless velocity component in R, ϕ and Z direction, x, y, z: Cartesian coordinate system (m), Z: Dimensionless axial coordinate, α: Thermal diffusivity (m^2/s), β: Volumetric thermal expansion coefficient (1/K), θ: Dimensionless temperature, ψr, ψϕ, ψz: Vector potential component in R,ϕ and Z – direction**,** FAI**:** angular direction**.**

Keywords
Laminar free convection, Al_2O_3 and TiO_2 nanofluids, porous media, horizontal annulus.

1. INTRODUCTION
The flows in porous media which is thermally driven have many applications fields as in chemical, mechanical and civil engineering. These applications include thermal insulation of buildings, drying processes, heat exchangers, nuclear reactors and solar collectors. Many applications can be found in books such as [1], [2] and [3]. In such engineering systems the conventional fluids (including oil, water and ethylene glycol mixture) have inherently poor thermal conductivity. The thermal conductivity of the particle materials, metallic or nonmetallic such as Al2O3 and TiO2 are higher than that of the conventional fluid so nanofluids of including these particles have high thermal conductivity and preferred in these applications.

[4] Numerically study the interplay between internal heat generation and externally driven natural convection inside a porous medium annulus. The domain which is axisymmetric bounded with adiabatic top and bottom walls and differentially heated side walls sustaining steady natural convection of a fluid with Prandtl number, Pr=5, through a porous matrix of volumetric porosity, ϕ=0.4. The solid–fluid thermal conductivity ratio is independently increased and the internal Rayleigh number increases proportionately when the permeability based external Rayleigh number.

[5] Studied numerically the natural heat transfer convection and conduction in a vertical annulus formed between an inner heat generating solid circular cylinder and an outer isothermal cylindrical boundary for laminar flow. Results are presented for the flow and temperature distributions and Nusselt numbers on different cross sectional planes and longitudinal sections for Rayleigh number ranging from 10^5 to 10^8, solid volume fraction of $0<\varphi<0.05$ with copper-water nanofluid as the working medium. The driven flow in the annular tube is strongly influenced by orientation of tube, so the study has been carried out for different inclination angles.

[6] Natural convection of nanofluids contained in a rectangular enclosure subject to uniform heat flux along the vertical sides was studied analytically and numerically. The research takes three types of nanoparticles into consideration that is Cu, Al_2O_3 and TiO_2. A good agreement is found between the analytical predictions and the numerical simulations.

Steady mixed convection boundary layer flow from an isothermal horizontal circular cylinder embedded in a porous medium filled with a nanofluid has been studied by [7] for both cases of a heated and cooled cylinder. Three different types of nanoparticles are considered, namely Cu, Al2O3 and TiO2. It is found that for each particular nanoparticle, as the nanoparticle volume fraction ϕ increases, the magnitude of the skin friction coefficient decreases, and this leads to an increase in the value of the mixed convection parameter λ which first produces no separation. On the other hand, it is also found that of all the three types of nanoparticles considered, for any fixed values of ϕ and λ, the nanoparticle Cu gives the largest values of the skin friction coefficient followed by TiO2 and Al2O3.

In the present paper, natural convection of two kinds of nanofluids of Al_2O_3 and TiO_2 particles with water as based fluid will be studied. The nanofluids flow in a cylindrical annular enclosure subject to uniform heat flux along the inner cylinder wall will be studied numerically. Two models of thermal conductivity will be taken in consideration. Model 1 will be Maxwell-Garnetts model and Model 2 is the Yu and Choi's correlation [6].

2. GOVERNING EQUATIONS

The effective thermal conductivity of the nano-fluid is approximated by Maxwell-Garnetts model [6]:

$$\frac{k_{nf}}{k_f} = \frac{k_s+2k_f-2\,\varphi\,(k_f-k_s)}{k_s+2k_f+\varphi\,(k_f-k_s)} \quad (1)$$

The use of this equation is restricted to spherical nano-particles where it does not account for other shapes of nano-particles. This model is found to be appropriate for studying heat transfer enhancement using nanofluid [7, 8].

The Yu and Choi's correlation [6]. This correlation includes the effect of a liquid nanolayer on the surface of a nanoparticle:

$$\frac{k_{nf}}{k_f} = \frac{k_s+2k_f-2\,\varphi\,(k_f-k_s)(1+\gamma)^3}{k_s+2k_f+\varphi\,(k_f-k_s)(1+\gamma)^3} \quad (2)$$

Where γ is the ratio of the nanolayer to the radius of the original particle. The value of γ is held fixed at 0.1.

The viscosity of the nano-fluid can be approximated as viscosity of a base fluid μ_f containing dilute suspension of fine spherical particles and is given by [8]:

$$\mu_{nf} = \frac{\mu_f}{(1-\varphi)^{2.5}} \quad (3)$$

The Pak and Cho's correlation which results from experimental measurement of mixtures consisting in ultra fine metallic oxide particles suspends in water [6]:

$$\mu_{nf} = \mu_f\,(1 + 39.11\varphi + 533.9\,\varphi^2) \quad (4)$$

The effective density of the nanofluid is given as:

$$\rho_{nf} = \varphi\rho_s + (1-\varphi)\,\rho_f \quad (5)$$

The heat capacitance of the nano-fluid is expressed as [5] and [8]:

$$(\rho\,C_p)_{nf} = \varphi\,(\rho\,C_p)_s + (1-\varphi)\,(\rho\,C_p)_f \quad (6)$$

The thermo physical properties of water at 300 K are given in Table (1).

Table 1. The thermo physical properties of water at 300 K

physical properties	Pure water
P(kg/m^3)	997.1
Cp(J/kg K)	4179
K(W/m K)	0.613
β (1/K)	21x10^{-5}

1.1 Mass Conservation

$$\frac{\partial\,u_r}{\partial r} + \frac{u_r}{r} + \frac{1}{r}\frac{\partial\,u_\emptyset}{\partial\emptyset} + \frac{\partial\,u_z}{\partial z} \quad (7)$$

1.2. Momentum Equations

The most common model used for flow in the porous media is the Darcy flow model. Darcy's law states that the volume average velocity through the porous material is proportional with the pressure gradient. In three dimensional flows, the Darcy's model [9] is:

1.2.1. Momentum Equation In Radial Direction

$$u_r = \frac{K}{\mu_{nf}}\left[-\frac{\partial p}{\partial r} - \rho_{nf}\,g\left[1-\beta_{nf}\,(T_1-T_2)\right]\cos\emptyset\right] \quad (8)$$

1.2.2. Momentum Equation In Angular Direction

$$u_\emptyset = \frac{K}{\mu_{nf}}\left[-\frac{\partial p}{\partial\emptyset} - \rho_{nf}\,g\left[1-\beta_{nf}\,(T_1-T_2)\right]\sin\emptyset\right] \quad (9)$$

1.2.3. Momentum Equation In Axial Direction

$$u_z = \frac{K}{\mu_{nf}}\left[-\frac{\partial p}{\partial z}\right] \quad (10)$$

1.2.4. Energy Equation

$$\frac{\partial\left(\rho_{nf}\,C_{p_{nf}}T\right)}{\partial t} + u_r\frac{\partial}{\partial r}\left(\rho_{nf}\,C_{p_{nf}}T\right) + \frac{u_\emptyset}{r}\frac{\partial}{\partial\emptyset}\left(\rho_{nf}\,C_{p_{nf}}T\right) + u_z\frac{\partial}{\partial z}\left(\rho_{nf}\,C_{p_{nf}}T\right) = \frac{1}{r}\frac{\partial}{\partial r}\left\{r\frac{\partial(k_{nf}T)}{\partial r}\right\} + \frac{1}{r^2}\frac{\partial^2(k_{nf}T)}{\partial\emptyset^2} + \frac{\partial^2(k_{nf}T)}{\partial\emptyset z^2} + \frac{\dot{q}}{(\rho\,C_p)_{nf}} + \mu\,\Phi \quad (11)$$

Where Φ is viscous dissipation function and will be neglected.

A vorticity vector Ω and a vector potential Ψ with its components are [10]:

$$\Psi = (\psi_r, \psi_\phi, \psi_z)$$

Defined by:

$$U = \alpha_f\,\nabla X\Psi \quad (13)$$

$$\nabla^2\psi_r = \frac{1}{R}\frac{\partial U_z}{\partial\emptyset} - \frac{\partial U_\emptyset}{\partial Z} \quad (14)$$

$$\nabla^2\psi_\emptyset = \frac{\partial U_r}{\partial Z} - \frac{\partial U_z}{\partial R} \quad (15)$$

$$\nabla^2\psi_z = \frac{1}{R}\frac{\partial(RU_\emptyset)}{\partial R} - \frac{1}{R}\frac{\partial U_r}{\partial\emptyset} \quad (16)$$

3. NON DIMENSIONAL VARIABLES

To convert the governing equations to the dimensionless form, the characteristic length for the present study is taken r_2 as in [11], the dimensionless magnitudes must be defined as follow:

$$R = \frac{r}{r_2}, Z = \frac{z}{r_2}, U_r = \frac{u_r\,r_2}{\alpha_{nf}}, U_\emptyset = \frac{u_\emptyset\,r_2}{\alpha_{nf}}, U_r = \frac{u_z\,r_2}{\alpha_{nf}}$$

$$\theta = 2\frac{k_{nf}\,(T-T_2)}{\dot{q}\,r_2^2}, P = \frac{p\,K}{\alpha_{nf}\,\mu_{nf}}, R_a^* = \frac{\dot{q}\;g\,\beta_f K r_2}{2\,k_{nf}\,\alpha_{f\,\vartheta}}$$

Substitute these dimensionless magnitudes in the governing equations. Alternative expressions of eq. (8) may be written in terms of $\psi_r, \psi_\phi\ and\ \psi_z$ as:

$$U_r = \frac{1}{R}\frac{\partial\psi_z}{\partial\emptyset} - \frac{\partial\psi_\emptyset}{\partial Z} \quad (17)$$

$$U_{\emptyset} = \frac{\partial \psi_r}{\partial Z} - \frac{\partial \psi_z}{\partial R} \quad (18)$$

$$U_r = \frac{1}{R}\frac{\partial (R\psi_{\emptyset})}{\partial R} - \frac{1}{R}\frac{\partial \psi_r}{\partial \emptyset} \quad (19)$$

Taking curl of momentum equations to eliminate pressure terms, the momentum equations will be:

$$R_a^* \Pr C_1 \left(\sin \emptyset \frac{\partial \theta}{\partial Z}\right) = -\frac{\partial^2 \psi_r}{\partial R^2} - \frac{1}{R^2}\frac{\partial (R\psi_r)}{\partial R} - \frac{2}{R}\frac{\partial \psi_r}{\partial R} - \frac{1}{R^2}\frac{\partial^2 \psi_r}{\partial \emptyset^2} - \frac{\partial^2 \psi_r}{\partial Z^2} - \frac{2}{R}\frac{\partial \psi_z}{\partial Z} \quad (20)$$

$$R_a^* \Pr C_1 \left(\cos \emptyset \frac{\partial \theta}{\partial Z}\right) = -\frac{\partial^2 \psi_{\emptyset}}{\partial Z^2} - \frac{1}{R^2}\frac{\partial^2 \psi_{\emptyset}}{\partial \emptyset^2} - \frac{\partial^2 \psi_{\emptyset}}{\partial R^2} + \frac{\psi_{\emptyset}}{R^2} - \frac{1}{R}\frac{\partial \psi_{\emptyset}}{\partial R} - \frac{2}{R^2}\frac{\partial \psi_r}{\partial \emptyset} \quad (21)$$

$$R_a^* \Pr C_1 \left(\frac{1}{R}\cos \emptyset \frac{\partial \theta}{\partial \emptyset} + sin\emptyset \frac{\partial \theta}{\partial R}\right)/\alpha_{nf} = -\frac{\partial^2 \psi_z}{\partial Z^2} - \frac{1}{R^2}\frac{\partial^2 \psi_z}{\partial \emptyset^2} - \frac{\partial^2 \psi_z}{\partial R^2} - \frac{1}{R}\frac{\partial \psi_z}{\partial R} \quad (22)$$

Where $C_1 = \frac{\alpha_f}{\alpha_{nf}}\left[(1-\varphi) + \varphi\frac{(\rho\,\beta)_s}{(\rho\,\beta)_f}\right](1-\varphi)^{2.5}$ (23)

And the energy equation will be:

$$\left(\frac{1}{R}\frac{\partial \psi_z}{\partial \emptyset} - \frac{\partial \psi_{\emptyset}}{\partial Z}\right)\frac{\partial \theta}{\partial R} + \frac{1}{R}\left(\frac{\partial \psi_r}{\partial Z} - \frac{\partial \psi_{\emptyset}}{\partial R}\right)\frac{\partial \theta}{\partial \emptyset} + \left(\frac{\psi_{\emptyset}}{R} - \frac{\partial \psi_{\emptyset}}{\partial R} - \frac{1}{R}\frac{\partial \psi_r}{\partial \emptyset}\right)\frac{\partial \theta}{\partial Z} = \alpha_{nf}\left[\frac{\partial^2 \theta}{\partial R^2} + \frac{1}{R}\frac{\partial \theta}{\partial R} + \frac{1}{R^2}\frac{\partial^2 \theta}{\partial \emptyset^2} + \frac{\partial^2 \theta}{\partial Z^2}\right] + 2\frac{(\rho\, C_p)_f}{(\rho\, C_p)_{nf}} \quad (24)$$

2.1. Dimensionless Hydraulic Boundary Conditions

For the vector potential field, the boundary conditions are given as:

$$\frac{1}{R}\frac{\partial (R\psi_r)}{\partial R} = \psi_{\emptyset} = \psi_z = 0 \quad at \quad R = R_1, L$$

$$\psi_r = \frac{\partial \psi_{\emptyset}}{\partial \emptyset} = \psi_z = 0 \qquad at \quad \emptyset = 0, \pi$$

$$\psi_r = \psi_{\emptyset} = \frac{\partial \psi_z}{\partial Z} = 0 \qquad at \quad Z = 0, L$$

2.2. Dimensionless Thermal Boundary Conditions

For the temperature field, the dimensionless thermal boundary conditions are:

$$\theta = 1 \qquad at\ R = R_1 = r_1/r_2$$

$$\theta = 0 \qquad at\ R = R_2 = 1$$

$$\frac{\partial \theta}{\partial \emptyset} = 0 \qquad at\ \emptyset = 0, \pi$$

$$\frac{\partial \theta}{\partial Z} = 0 \qquad at\ Z = 0, L$$

Now the equations (20, 21, 22 and 24) were transformed into the finite difference equations, where the upwind differential method in the left hand side of the energy eq.(24) and the centered – space differential method for the other terms were used, and solved by using (SOR) method [10]. A computer program was built using MATLAB program to meet the requirements of the problem. It is clear that as the grid becomes finer, the convergence of the results becomes better. It seems to be reasonable to take the number of grid points as 21 grid points in the R – direction, 31 in the ϕ – direction and 301 in the Z – direction.

4. CALCULATION OF LOCAL AND AVERAGE NUSSELT NUMBER

Local Nusselt number is the dimensionless parameter indicative of the rate of energy convection from a surface and can be obtained as follows [12]:

$$Nu = \frac{q(r_2 - r_1)}{k(T_1 - T_2)} \quad (25)$$

The local Nusselt number Nu_1 and Nu_2 on the inner and the outer cylinders are written in the form:

$$Nu = -(1-R_1)\frac{k_{nf}}{k_f}\left(\frac{\partial \theta}{\partial R}\right)_{R=R_1} \quad (26)$$

$$Nu = -(1-R_1)\frac{k_{nf}}{k_f}\left(\frac{\partial \theta}{\partial R}\right)_{R=L} \quad (27)$$

The average Nusselt number Nu_{in} and Nu_{out} on the inner and the outer cylinders are defined as:

$$Nu_{in} = -(1-R_1)\frac{k_{nf}}{k_f}\frac{1}{\pi L}\int_0^L\int_0^{\pi}\left(\frac{\partial \theta}{\partial R}\right)_{R=R_1} d\emptyset\, dZ \quad (28)$$

$$Nu_{in} = -(1-R_1)\frac{k_{nf}}{k_f}\frac{1}{\pi L}\int_0^L\int_0^{\pi}\left(\frac{\partial \theta}{\partial R}\right)_{R=L} d\emptyset\, dZ \quad (29)$$

5. RESULTS and DISCUSSION

5.1. Local and Average Nusselt Number

Distribution of local Nusselt number along the length of the cylinder is illustrated in Fig. 2 to Fig. 7 for different Rayleigh number and nanoparticles volume fraction. Comparing Fig. 3 and Fig. 4 show that for the same value of the modified Raleigh number (Ra^*=500), the local Nu number is reached a maximum value equal to 4.25 and then decrease and fixed at a value of 4.182 for pure water while adding Al_2O_3 particles of 0.5 percent volume fraction cause to increase the value to 4.988 for model 1 and to 4.542 for model2. Adding 0.5 percent of TiO_2 particles cause to increase the value of the local Nu number to 4.128 for model 1 and to 3.748 for model 2 as shown in Fig, 6 and Fig. 7 respectively.

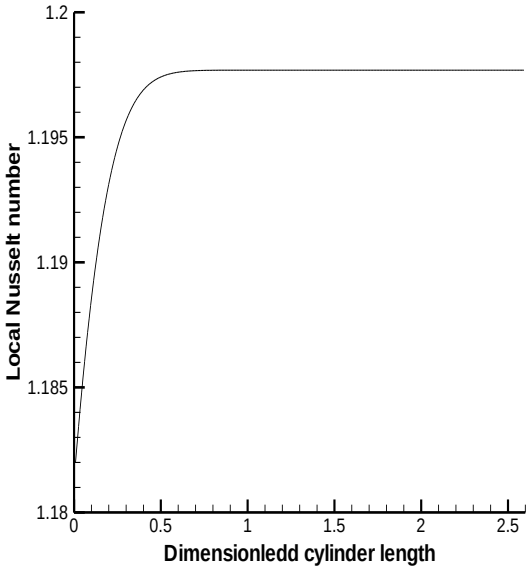

Fig. 2: Local Nu along cylinder length for pure water model 1 Ra=10

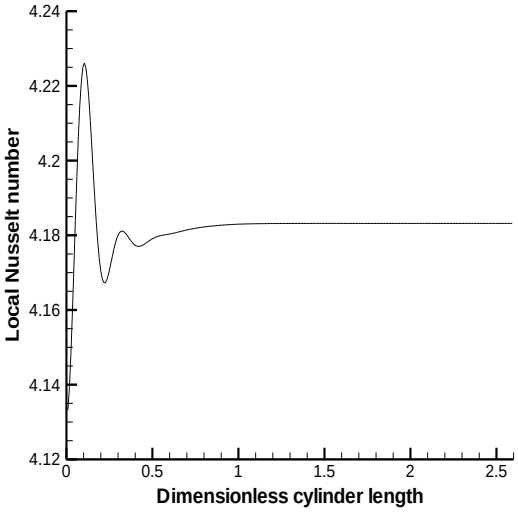

Fig. 3: Local Nu along cylinder length for pure water model 1 Ra=500

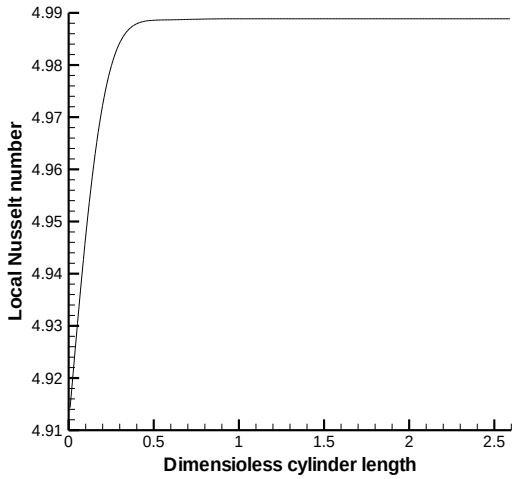

Fig. 4: Local Nu along cylinder length for Al_2O_3 model 1 Ra=500 and φ=0.5

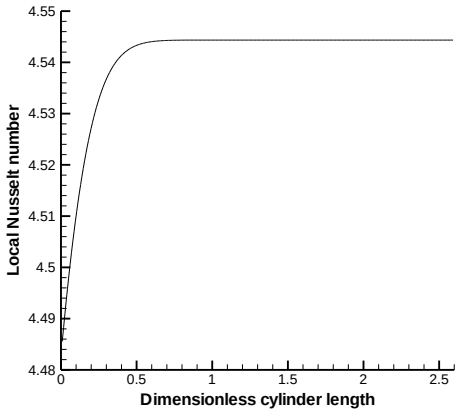

Fig. 5: Local Nu along cylinder length for Al_2O_3 model 2 Ra=500 and φ=0.5

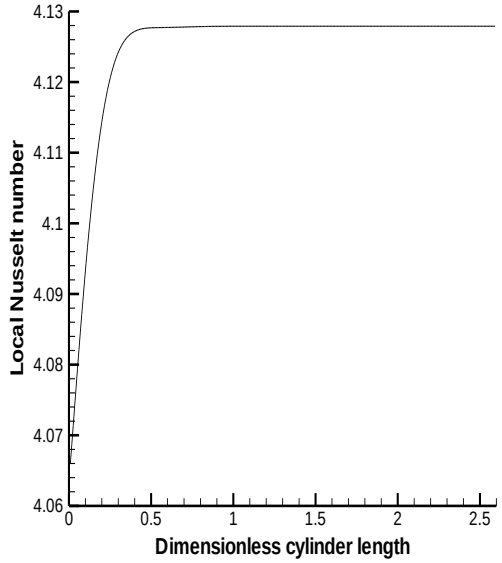

Fig. 6: Local Nu along cylinder length for TiO_2 model 1 Ra=500 and φ=0.5

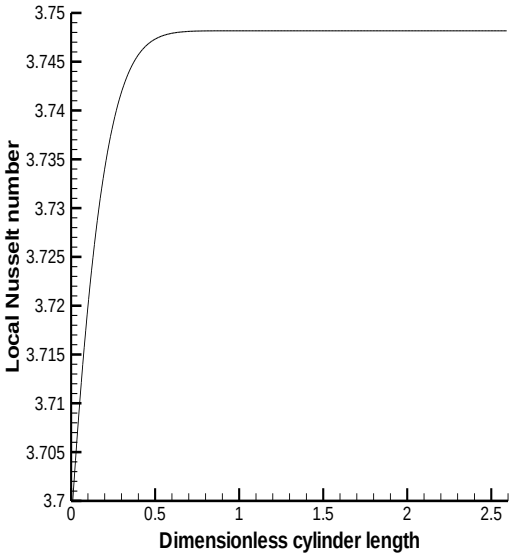

Fig. 7: Local Nu along cylinder length for TiO_2 model 2 Ra=500 and φ=0.5

5.2. Effect of Modified Rayleigh number and Other Parameters

Fig. 8 and Fig. 9 show the variation of the average Nusselt number on the hot and cold cylinders respectively with Ra^* for different volume fractions of Al_2O_3. Model 1 in Fig. 8 shows a maximum value of the average Nu of 18.0007 for φ=0.5 and Ra^* =500, while Nu equal 5.004 for model 2 as shown in Fig. 9.

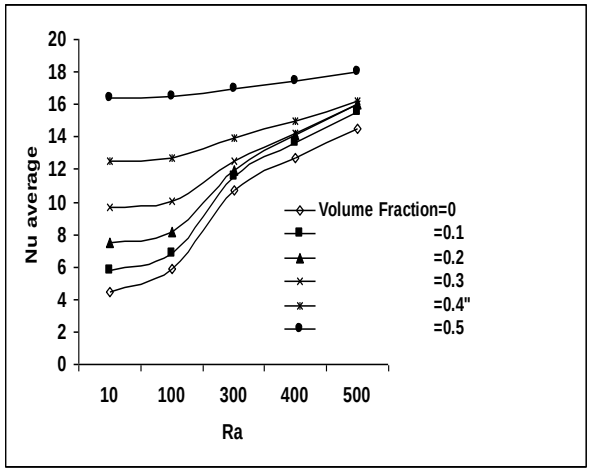

Fig. 8: The variation of the average Nu with modified Ra on the hot cylinder for Al_2O_3 model 1

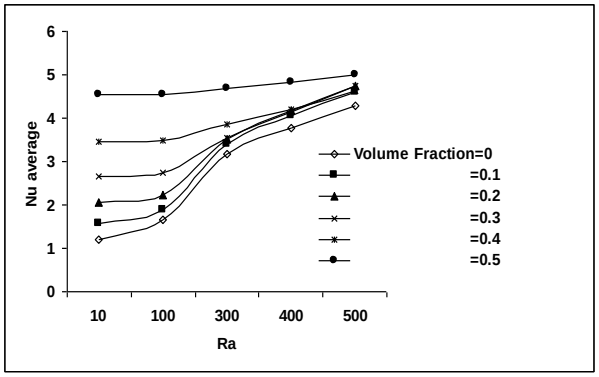

Fig. 9: The variation of the average Nu with modified Ra on the cold cylinder for Al_2O_3 model 1

Fig. 10 and Fig. 11 show the variation of the average Nusselt number on the hot and cold cylinders respectively with Ra^* for different volume fractions of TiO_2. Model 1 in Fig. 10 shows a maximum value of the average Nu of 16.446 for φ=0.5 and Ra^*=500, while Nu equal 4.54 for model 2 as shown in Fig. 9.

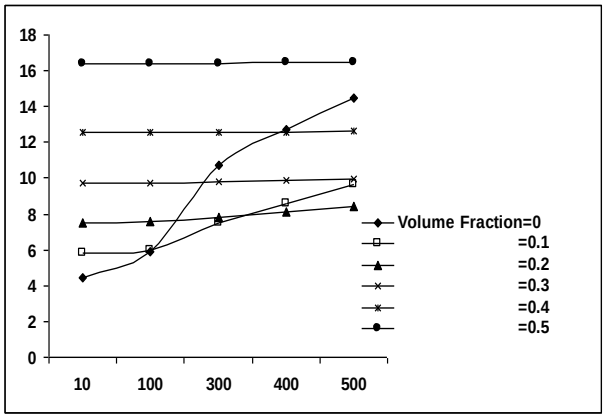

Fig. 10: The variation of the average Nu with modified Ra on the hot cylinder for Al_2O_3 model 2

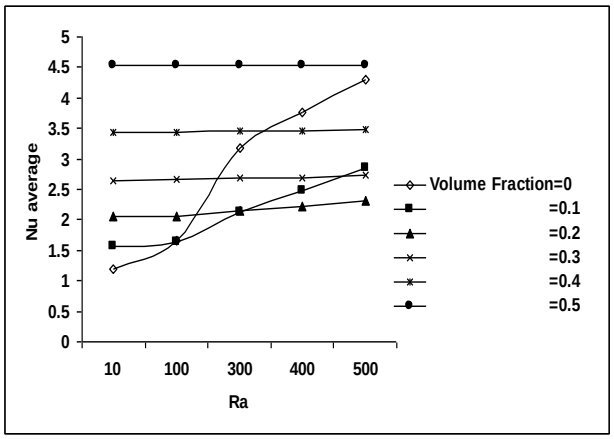

Fig. 11: The variation of the average Nu with modified Ra on the cold cylinder for Al_2O_3 model 2

Fig. 12 shows a comparison of the variation of the average Nu with the modified Ra^* on the hot cylinder for the pure water and Al_2O_3 nanofluid of φ=0.5 for the two models, while Fig. 13 shows a comparison of the variation of the average Nu with the modified Ra^* on the hot cylinder for the pure water and TiO_2 nanofluid of φ=0.5 for the two models.

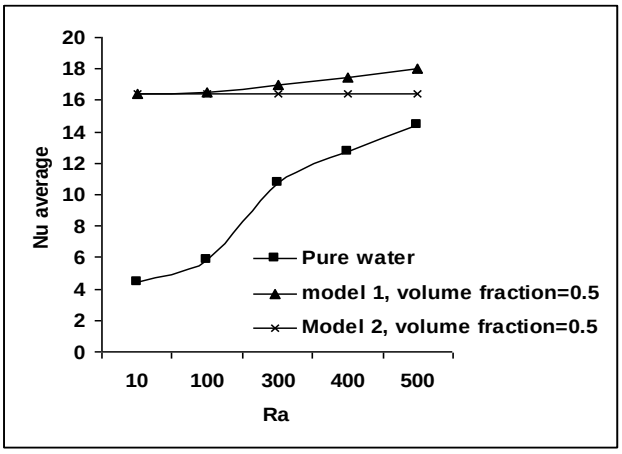

Fig. 12: Models comparison for the variation of the average Nu with modified Ra on the hot cylinder for Al_2O_3 nanofluid

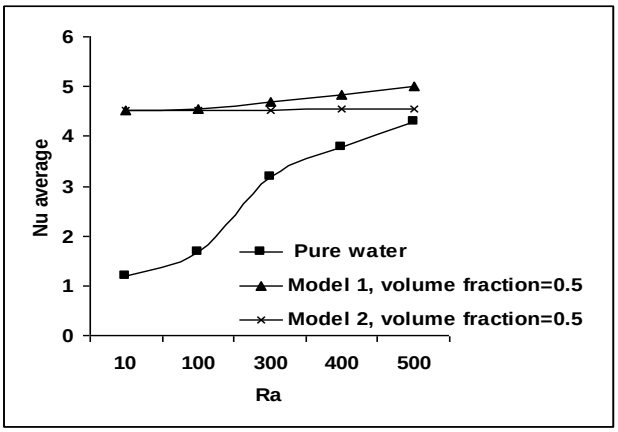

Fig. 13: Models comparison for the variation of the average Nu with modified Ra on the cold cylinder for Al_2O_3 nanofluid

The previous figures show that model 1 which consider the particles as a sphere is better than model two and adding Al_2O_3 particles with φ=0.5 cause to increase the average Nu 24.57% than that in pure water for Ra^*=500 and adding TiO_2 particles with φ=0.5 cause to increase the average Nu 16.488% than that in pure water for Ra^*=500. So the deviation in increasing the average number (which gives an indication of increasing the heat transfer) between adding Alumina or Titania is 8.082% and in the present study it is recommended to add the Alumina particles and the experimental study will consolidate these results.

Correlations are obtained for Al_2O_3 and TiO_2 nanofluids model 1 as follow:

For Al_2O_3 nanofluid: $Nu = 1.594\ Ra^{*0.17}\varphi^{2.57}$

For TiO_2 nanofluid: $Nu = 1.405\ Ra^{*0.171}\varphi^{1.75}$

6. CONCLUSIONS

The following major conclusions can be drawn from the study:

1- The local Nu number is reached a maximum value equal to 4.25 the decrease and fixed at a value of 4.182 for pure water while adding Al_2O_3 particles of 0.5 percent volume fraction cause to increase the value to 4.988 for model 1 and to 4.542 for model2.

2- Adding 0.5 percent of TiO_2 particles cause to increase the value of the local Nu number to 4.128 for model 1 and to 3.748 for model 2.

3- A maximum value of the average Nu of 18.0007 for Al_2O_3 nanofluid of model 1 and 5.004 for model 2 is obtained for φ=0.5 and Ra^* =500.

4- A maximum value of the average Nu of TiO_2 nanofluid is equal 16.446 for model1 with φ=0.5 and Ra^* =500, while Nu equal 4.54 for model 2

5- This study can be done in the future using copper or copper oxide as nanoparticles to compare it with present research.

7. REFERENCES

[1] Pop, D.B. Ingham, Convective Heat Transfer: Mathematical and Computational Modeling of Viscous Fluids and Porous Media, Pergamon, Oxford, 2001.

[2] Vafai, K., Handbook of Porous Media. 2nd edn. Taylor and Francis, New York (2005)

[3] Nield D.A., Bejan A., Convection in Porous Media, third ed., Springer, New York, 2006.

[4] Reddy B.V.K., Arunn Narasimhan, 2010," Heat generation effects in natural convection inside a porous annulus, International Communications in Heat and Mass Transfer 37 (2010) 607–610

[5] Mina Shahi, Amir Houshang Mahmoudi, Farhad Talebi, 2011," A numerical investigation of conjugated-natural convection heat transfer enhancement of a nanofluid in an annular tube driven by inner heat generating solid cylinder, International Communications in Heat and Mass Transfer 38 (2011) 533–542

[6] Alloui Z., Vasseur P., Reggio M., 2012," Analytical and numerical study of buoyancy-driven convection in a vertical enclosure filled with nanofluids", Heat Mass Transfer (2012) 48:627–639

[7] Nazar R., Tham L., Pop I., Ingham D. B., 2011," Mixed Convection Boundary Layer Flow from a Horizontal Circular Cylinder Embedded in a Porous Medium Filled with a Nanofluid", Transp Porous Med (2011) 86:517–536.

[8] Esmaeilpour M., Abdollahzadeh M., Free convection and entropy generation of nanofluid inside an enclosure with different patterns of vertical wavy walls, International Journal of Thermal Science 52 (2012)127-136.

[9] Wang Bu – Xuan and Zhang Xing, "Natural Convection in Liquid Saturated Porous Media Between Concentric Inclined Cylinders" Int. J. Heat and Mass Transfer Vol. 33. No 5, pp. 827-833, 1990.

[10] Aziz K. and Hellums J. D., Numerical Solution of the Three Dimensional Equations of Motion for Laminar Natural Convection, The Physics of Fluids, V0l. 10, No. 2, pp. 314 – 324, 1967

[11] Al- Hafidh Manal, Haithem H. Muhammad, Ban B. Jawad, 2014,"Effect of Angle of Rotation for Fiber Aligned in a Composite Material Wall of Inclined Enclosure on Heat Transfer", International Journal of Computer Applications, Volume 92 – No.12, 975 – 8887April.

[12] Hakan F. Oztop, Eiyad Abu-Nada," Numerical study of natural convection in partially heated rectangular enclosures filled with nanofluids", International Journal of Heat and Fluid Flow, Vol. 29, pp. 1326- 1336, 2008.